Plant, Cell & Environment

Plant, Cell and Environment (2010) **33**, 1161–1175 doi: 10.1111/j.1365-3040.2010.02137.x

Exploring the soluble proteome of Tobacco Bright Yellow-2 cells at the switch towards different cell fates in response to heat shocks

MILENA MARSONI[1], CARLO CANTARA[1], MARIA CONCETTA DE PINTO[2], COSIMO GADALETA[2], LAURA DE GARA[2,3], MARCELLA BRACALE[1] & CANDIDA VANNINI[1]

[1]*Dipartimento Ambiente Salute Sicurezza, Università degli Studi dell'Insubria, via G. B. Vico 46, 21100 Varese, Italy,*
[2]*Dipartimento di Biologia e Patologia Vegetale, Università degli Studi di Bari, via E. Orabona 4, 70125 Bari, Italy and*
[3]*Centro Integrato di Ricerca, Università Campus Bio-Medico di Roma, via A. del Portillo 21, 00128 Roma, Italy*

ABSTRACT

Tobacco (*Nicotiana tabacum*) Bright Yellow-2 (TBY-2) cells undergo different fates when exposed for 10 minutes to heat stresses of different severity. A 35 °C treatment causes a homeostatic response (HRE) allowing cells to cope with the stress; 55 °C triggers processes leading to programmed cell death (PCD), which is complete after 72 h. We have used a proteomic approach to gain insight into the molecular mechanisms defining the fate of TBY-2 cells induced by these two heat stresses. Tandem mass spectrometry (MS/MS) and two-dimensional electrophoresis (2-DE) analysis revealed little overlap of differentially-accumulated proteins: the different severities of heat treatment induced the modulation of specific proteins, some of which are responsible for different cell fates. When the imposed heat shock is beyond a certain threshold, the overall reduced metabolism may be the result of a series of events involving gene expression and oxidative damage that would lead to PCD. Our data suggest that the down-accumulation of several proteins involved in cellular redox homeostasis could provide, until now, an unappreciated contribution to understanding how many partners are involved in promoting the redox impairment leading to PCD. Moreover post-translational modifications seem to play important regulatory roles in the adaptation of TBY-2 cells to different intensities of heat stress.

Key-words: 2-DE; heat stress; mass spectrometry; plant cell death; redox homeostasis.

INTRODUCTION

Climate change is projected to induce relevant increases in temperature and alterations of the precipitation profile over the planet, with more robust alterations in the Mediterranean basin than in many other regions (Bates *et al.* 2008). Because of the global increases in atmospheric temperature, plants are expected to be forced to cope with heat stress conditions in wider and wider areas of our planet. Fluctuating or constantly over-optimum temperatures affect plant growth and development and pose a serious threat to worldwide crop production (Porter & Semenov 2005; Challinor *et al.* 2009). Heat-stress response appears to be one of the most conserved defense mechanisms present in all living organisms. Heat stress induces different kinds of metabolic responses, some of which seem to be activated under a plethora of unfavourable conditions and are aimed at maintaining cellular functionality (Desikan *et al.* 2001; Baniwal *et al.* 2004; Baena-González & Sheen 2008). It has been recently reported that heat shock also induces programmed cell death (PCD) in plants (Vacca *et al.* 2004). PCD is a highly regulated mechanism playing a pivotal role in eukaryotes during their development and in their response to biotic and abiotic factors (Gadjev *et al.* 2008). It is a genetically-defined process associated with distinctive cytological hallmarks including cytoplasm shrinkage, DNA fragmentation, plasma membrane blebbing and the formation of apoptotic bodies (Mittler & Lam 1995; Wang *et al.* 1996; Scott & Logan 2008).

Because of their uniformity, accessibility and reduced complexity, cell cultures are an attractive system in which to study the heat stress response. The aim of the present study was to investigate the molecular mechanisms involved in the response to heat stress in tobacco (*Nicotiana tabacum*) Bright Yellow-2 (TBY-2) cell suspension cultures. In particular, cells were exposed to two different heat shocks (HSs): 55 and 35 °C, for 10 min. HS at 55 °C is able to trigger PCD without addition of any PCD inducer (Vacca *et al.* 2004; Burbridge *et al.* 2007). In TBY-2 cells exposed to 55 °C, cell viability starts decreasing after 2 to 3 h of recovery at 27 °C, falls to 50% after 24 h and is negligible after 72 h (Vacca *et al.* 2004). The evidence that cell death occurs by PCD is provided by the presence of cytological hallmarks: cytoplasm shrinkage in 72% of 24 h-PCD cells, DNA laddering, and cytochrome c release from mitochondria (Locato *et al.* 2008). Moreover, 55 °C HS induces a biphasic production of H_2O_2 and a rapid increase in nitric oxide, two events necessary for the activation of PCD (Delledonne

Correspondence: M. Marsoni. Fax: + 39 0332 421390; e-mail: milena.marsoni@uninsubria.it

et al. 1998). In contrast, 35 °C HS leads to only a transient increase in H_2O_2 and a consequent alteration in reactive oxygen species (ROS) scavenging systems aimed at maintaining the cell redox homeostasis (Locato *et al*. 2008). We performed proteomic analysis of TBY-2 cells collected 3 and 6 h after HS exposure. These durations were chosen on the basis of previous results obtained in the same experimental setup (Locato *et al*. 2008). Three hours after 55 °C HS (3 h-PCD), the biochemical pathways leading to PCD have just been activated and the cytological evidence of cell death begins to be visible; six hours after the 55 °C HS (6 h-PCD), the increase in cell death is much more evident even at the cytological level. In the TBY-2 cells exposed to 35 °C HS, the homeostatic response (HRE) is at its highest levels between 3 and 6 h after treatment (3 h- and 6 h-HRE) and then returns to the control levels (Locato *et al*. 2008).

Proteomic analysis provides a robust and reliable approach to simultaneously study multiple signalling pathways. The data presented here reveal a great divergence in the number and kinds of proteins differentially accumulated in TBY-2 cells following the two different heat treatments. Several factors have been highlighted whose roles in homeostatic and PCD responses induced by heat stress was until now unappreciated.

MATERIALS AND METHODS

Cell culture, growth conditions and heat treatments

The suspension of TBY-2 cells was cultured at 27 °C as previously described (de Pinto *et al*. 2002). For heat shock, a stationary culture was diluted 4:100 (v/v; 100 mL), cultured for 4 d and then transferred for 10 min into a water bath at 35 °C or 55 °C, with constant shaking. After this treatment, the cells were returned at 27 °C for 3 and 6 h and then collected, frozen in liquid nitrogen and stored at –80 °C. Where indicated, spermidine 0.5–1.5 mM was added to the cell suspension 15 min before the HS exposition. Cell viability was measured by Trypan Blue staining as previously described (de Pinto *et al*. 2002). Three biological replicate were done.

Protein extraction and 2-D gel electrophoresis

The total proteins were extracted by phenol as previously described (Marsoni *et al*. 2008). The washed pellets were air-dried and recovered in 7 M urea, 2 M thiourea, 4% CHAPS, 50 mg mL^{-1} DTT, 0.5% of carrier ampholyte. Protein concentration was determined by Bradford assay (Sigma-Aldrich Italia, Milan, Italy). Three independent protein extractions were performed from each sample. Six hundred micrograms of total proteins were loaded onto an 18 cm and pH 4–7 linear gradient IPG strips (GE Healthcare, Uppsala, Sweden). Then IEF was performed at 16 °C in the IPGphor system (Amersham Biosciences, Uppsala, Sweden) as the following: for 4 h at 200 V, from 200 to 3500 V in gradient during 30 min, 3 h at 3500 V, from 3500 to 8000 V in gradient during 30 min, after which the run was continued at 8000 V to give a total of 70 kVh. Each focused strip was equilibrated for 30 min against 6 M urea, 30% glycerol, 2% sodium dodecyl sulphate (SDS), 50 mM Tris-HCl pH 8.8, 2% DTT and then a further 30 min with the substitution of the DTT with 2.5% iodoacetamide. The separation of proteins in the second dimension was performed with sodium dodecyl sulphate–polyacrylamide gel electrophoresis (SDS–PAGE) (12.5%) on an Ettan DALT System (GE Healthcare). The SDS–PAGE gels were visualized by the modified Colloidal Coomassie Brilliant Blue staining method (Aina *et al*. 2007). Each separation was repeated 3 times for each biological replicate to ensure the protein pattern reproducibility.

Image acquisition and spot detection

The gels were analysed by using the Image Master 2D Platinum software version 5.0 (Amersham Biosciences). Data were normalized by expressing protein abundance as percent spot volume relative to volume of total protein in the gel (% vol). The 2D gels for each biological replicate were averaged and the resulting gel (master gel) contains only the spots present in all of the gels. Statistical analysis (Student's *t*-test at a level of 95%) identified proteins that significantly increased or decreased (at least 1.5-fold in relative abundance) after the different treatments with respect to the control. These spots were selected for MS/MS analysis.

In-gel digestion and mass spectrometry analysis

Selected spots were manually excised from the 2D gels, washed twice and stored in 50% ethanol at 4 °C until digestion. Spots digestion was performed as previously described (Marsoni *et al*. 2008). The extracted tryptic fragments were analysed by MS/MS after reverse phase separation of peptides [liquid chromatography–electrospray ionization mass tandem spectrometry (LC-ESI-MS/MS)]. For all experiments, a Finningan LXQ linear ion trap mass spectrometer, equipped with a Finningan Surveyor MS plus HPLC system (Thermo Electron Corporation, CA, USA) was used. Chromatography separations were conducted on a BioBasic C18 column (150 μm internal diameter × 150 mm length and 5 μm particle size; Thermo Electron Corporation), using a linear gradient from 5 to 75% acetonitril, containing 0.1% formic acid, for 50 min. with a flow of 2 μL min^{-1}. Acquisitions were performed in the data-dependent MS/MS scanning mode (full MS scan range of 400–1400 m z^{-1} followed by Zoom scan for the most intense ion from the MS scan and full MS/MS for the most intense ion from the zoom scan), thus enabling a dynamic exclusion window of 3 min. Protein identification was performed by searching in the National Center for Biotechnology Information (NCBI) viridiplantae and/or EST-viridiplantae protein database using the MASCOT program (http://www.matrixscience.com). The following parameters were adopted for database searches:

complete carbamidomethylation of cysteines, partial oxidation of methionines, peptide mass tolerance 1.2 Da, fragment mass tolerance 0.8 Da and missed cleavage 1. For positive identification, the score of the result of [$-10 \times \log(P)$] had to be over the significance threshold level ($P > 0.05$). Unsuccessful protein identifications were submitted to de novo analysis by PepNovo software using default parameters (http://peptide.ucsd.edu/pepnovo.py). Only those PepNovo results were accepted that received a mean probability score of at least 0.5. Peptides sequences candidates were edited according to MS BLAST rules and MS BLAST search was performed against NCBI non-redundant database at http://www.dove.embl-heidelberg.de/Blast2/msblast.html. Statistical significance of hits was evaluated according to MS BLAST scoring scheme. Other than Molecular Weight Search (Mowse) and MS BLAST scoring system to assign correct identification we make a point of a minimum of two matched peptides.

For the subcellular localization we used CELLO v.2.5: subcellular localization predictor (Yu *et al*. 2006).

Semiquantitative RT-PCR experiments

Total RNA was extracted using the TRIzol reagent (Invitrogen, Carlsbad, CA, USA) according to the manufacturer's instructions. First-strand cDNA was synthesized from 2 μg of total RNA by using Superscript III reverse transcriptase (Invitrogen). PCR primers and the thermal cycling parameters for each gene were listed in Supporting Information Table S1. The 18S RNA was used as the inner control. The PCR products were isolated by 1% gel electrophoresis. The data were analysed with ImageJ 1.41 (http://rsb.info.nih.gov/ij/). All experiments were repeated three times.

Western blotting

Total soluble proteins were extracted by phenol method, as previously described, but after acetone precipitation the pellet was re-suspended in Laemmli sample buffer. 75 μg of proteins were loaded onto 14% SDS–PAGE gel and transferred to PVDF membranes (Westran CS, 0.45 μm, Whatman). Membranes were probed with 1:2000 AtSUMO1 antibody (Abcam, Cambrige, UK), using the Supersignal West Dura Extended Duration Chemiluminescent Substrate for HRP system (Pierce). Protein loading was verified by Ponceau staining of the membrane. The analysis was done in triplicate; however, only one representative Western blot is shown.

Ascorbate peroxidise activity

Cells were ground in liquid nitrogen and homogenized at 4 °C in extraction buffer [50 mM Tris-HCl pH 7.8, 0.05% (w/v) cysteine, 0.1% (w/v) bovine serum albumin and 1 mM ASC]. Homogenates were centrifuged at 20 000 *g* for 15 min and the supernatants used for spectrophotometric analysis. The activity of ascorbate peroxidase (APX; L-ascorbate: hydrogen peroxide oxidoreductase, EC 1.11.1.11) was tested according to de Pinto *et al*. (2002).

Statistical analysis

For all analysis at least three replicates were performed for each heat treatment and the values represent the means ($\pm$SD). Statistical analysis was done using a two-tailed Student's *t*-test and in the figures the symbols (*) and (**) indicate values that are significantly different with $P < 0.05$ and $P < 0.01$, respectively.

RESULTS

Heat response

TBY-2 cell cultures exposed to heat shocks at 35 and 55 °C for 10 min were analysed for cell viability. The decrease in cell viability 3 and 6 h after 55 °C HS was 15 and 25%, respectively, and a further decrease occurred in the following hours as has been previously reported (Vacca *et al*. 2004). In a substantial number of cells, cytoplasmic shrinkage was also evident confirming that PCD was triggered, consistent with data obtained previously under the same experimental conditions (Vacca *et al*. 2006). On the other hand, cell viability was not affected at 3 or 6 h after 35 °C HS.

2-D separation and identification of differentially-accumulated proteins in control and heat-treated TBY-2 cells

Total soluble proteins were isolated from cells that were heated at 35 or 55 °C for 10 min and then recovered after either 3 or 6 h at 27 °C. The amount of total extracted protein was not significantly different between the control and HS-exposed cells after phenolic extraction and during the time of the analysis here performed (data not shown). The protein extracts were subjected to IEF on a linear gradient ranging from pH 4 to 7 and were subsequently separated on 12.5% SDS–PAGE gels. Image analysis revealed an average of about 1000 reproducible protein spots in each gel stained with colloidal CBB (Fig. 1).

Image Master 2D Platinum software showed 116 protein spots that were changed significantly (*t*-test; $P < 0.05$) in relative abundance (at least 1.5-fold between control and heat treated cells). Ninety-four of these spots were successfully identified by LC–MS/MS analysis (Table 1).

Some of the identified proteins showed a discrepancy with their theoretical *M*r or p*I*. However, these kinds of phenomena are commonly found in 2-D gels for several reasons including modification of proteins during the extraction or the separation procedure, different isoforms derived from various genes, proteolytic cleavage, or post-translational modifications (PTMs). Cross-species protein identification can also produce this variation.

As shown in Table 1 and Fig. 2, among the 94 proteins identified, 17 proteins were differentially-accumulated in 3 h-HRE cells compared with the control. Five different proteins had changed in 6 h-HRE cells relative to control, indicating cell recovery and late responses to the heat shock treatment. At 55 °C, the situation changed dramatically: 48

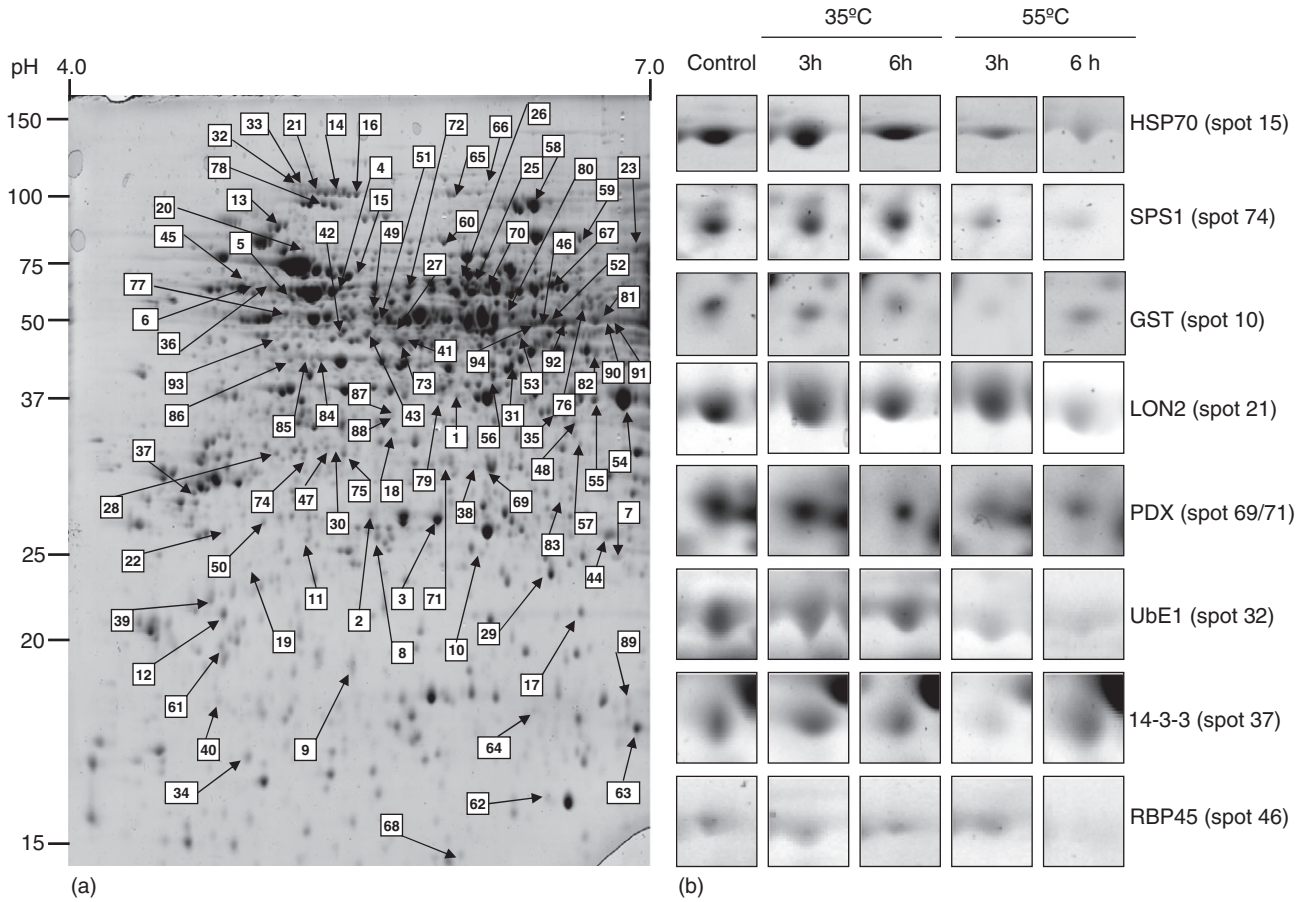

Figure 1. Images of Colloidal Coomassie Brilliant Blue-stained 2D isoelectric focusing sodium dodecyl sulphate–polyacrylamide gel electrophoresis (IEF SDS–PAGE) gels. (a) Image of a representative gel: spots differently expressed are indicated by their relative numbers. (b) Selected differentially accumulated protein spots in tobacco Bright Yellow-2 (TBY-2) cells exposed to different heat shocks.

and 55 proteins were differentially-expressed compared with the control in 3 h-PCD and 6 h-PCD, respectively.

Following the procedures of Bevan *et al*. (1998), the identified proteins were sorted into different functional categories as follows: disease/defence (19); protein synthesis and fate (16); signal transduction/regulation (13); metabolism (31); secondary metabolism (4); and cell structure (11). As shown in Fig. 2, in HRE-cells the differentially-expressed proteins are equally distributed between up- and down-accumulation, whereas in PCD cells the number of down-accumulated proteins is double that of up-regulated proteins. The down-accumulated proteins in PCD cells mainly belong to the disease/defence, protein synthesis/fate and metabolism categories.

Validation of proteomic results with other approaches

Semiquantitative RT-PCR analysis

Semiquantitative RT-PCR analyses were performed to detect the level of expression of eight genes corresponding to proteins that were found to be differentially-accumulated in PCD cells and which belonged to four different functional categories. As shown in Fig. 3, significant accumulation differences at the protein level were confirmed at the mRNA level for *HSP70 homolog*, *14-3-3 like protein B*, *ubiquitin-activating enzyme E1* and *glutatione-S-transferase*. For the other genes (*Lon2 protease*, *pyridoxine biosynthesis*, *spermidine synthase and RBP45*) the correspondence between mRNA and protein levels is less stringent. In spite of the differences in the entity of the changes as revealed by the two experimental approaches, in all the cases the alterations in protein levels and gene expression were in the same direction.

Western blot analysis of small ubiquitin-like modifier (SUMO) proteins

Two-dimensional gel electrophoresis (2-DE) data indicate a decrease in the SUMO1 protein (spot 34) in 6 h-PCD cells. We used immunoblot analysis with AtSUMO1 antibody to detect free and conjugated forms in soluble cellular extracts (Fig. 4). In control and 6 h-HRE cells, the anti-SUMO antibody recognized an abundant species that co-migrated with SUMO1. In addition, a heterogeneous smear of higher molecular mass proteins was also detected, that represented SUMO-conjugated proteins. On the other hand, 6 h after

Table 1. List of proteins identified by MS/MS in heat-treated TBY-2 cells

Spot	Protein name	NCBI accession number	35 °C		55 °C		Loc.	MS/MS (Mascot)		MW (Da)/pI	
			3 h	6 h	3 h	6 h					
			Fold-of variation versus control					Pept./score		Theor.	Exp.
Disease/defence											
1	Aldo/keto reductase[a] (*N. tabacum*)	gi|190734152	=	=	–1.6	=	C	3	182	37.4/5.7	36.0/5.9
2	Ascorbate peroxidase (*N. tabacum*)	gi|559005	1.5	=	–2	=	C	3	125	27.3/5.4	27.0/5.4
3	Ascorbate peroxidase[a] (*N. tabacum*)	gi|76869309	=	=	–1.5	–1.5	C	9	441	27.0/5.4	27.0/5.9
4	Cpn60 β (*N. tabacum*)	gi|190751099	=	1.5	=	1.7	Ch	3	201	64.2/5.7	62.0/5.6
5	Cpn60 β ATP binding protein (*S. tuberosum*)	gi|1762130	=	=	=	1.9	Ch	4	154	63.8/5.7	62.0/5.2
6	Cpn60 α subunit[a] (*N. tabacum*)	gi|190794529	=	=	=	1.7	Ch	3	220	53.2/5.2	62.0/5.0
7	Dehydroascorbate reductase (*N. tabacum*)	gi|28192427	=	=	–1.5	–1.7	C	2	75	23.6/7.7	23.8/6.7
8	Ferritin-1[a] (*N. sylvestris*)	gi|48754322	=	=	=	–1.9	Ch	2	128	28.2/5.7	26.0/5.6
9	Glutaredoxin family[a] (*S. tuberosum*)	gi|146443624	=	–1.8	=	–1.7	M	3	106	18.7/5.9	15.2/5.3
10	Glutathione S-transferase PARB (*N. tabacum*)	gi|232202	=	=	–1.8	=	C	4	182	24.0/5.5	25.0/6.0
11	Glutathione S-transferase, putative[a] (*N. tabacum*)	gi|76869824	=	=	=	–2	C	3	129	24.0/5.3	25.0/5.2
12	Mitochondrial small heat shock protein (*S. lycopersicum*)	gi|3492854	1.5	=	=	=	M	2	92	23.8/6.5	22.0/4.8
13	Heat-shock protein 90, putative (*A. thaliana*)	gi|6466963	=	=	=	–1.8	M	3	140	91.2/5.2	90.0/5.1
14	Homolog to heat-shock protein, putative[a] (*N. tabacum*)	gi|92027886	=	=	=	–2	C/N	6	262	94.0/5.2	110/5.5
15	Homolog to HSP70 mitochondrial precursor (*P. vulgaris*)	gi|399940	=	=	=	–2.2	M	5	260	72.5/6.0	72.0/5.5
16	HSP70[a] (*N. tabacum*)	gi|92037393	=	=	–1.6	–2.0	C/N	4	227	93.6/5.2	110/5.6
17	Methionine sulfoxide reductase[a] (*N. tabacum*)	gi|76868425	=	=	=	–1.8	C/N	6	374	23.0/6.1	22.0/6.6
18	NADPH dependent thioredoxin reductase (*C. reinhardtii*)	gi|159488145	1.7	=	=	=	C	2	85	36.7/5.3	33.0/5.6
19	Thioredoxin peroxidase (*N. tabacum*)	gi|21912927	=	=	=	–4.3	Ch	4	168	30.0/8.2	24.0/5.0
Protein synthesis and fate											
20	Acyl-peptide hydrolase-like[b] (*P. sitchensis*)	gi|116789192	=	=	=	2.3	Ch	2	98	80.7/5.3	80.0/5.4
21	ATP-dependent proteinase Lon2, putative (*O. sativa*)	gi|50508109	=	=	=	–1.9	M	2	107	110.1/5.3	110/5.4
22	Cysteine protease (*N. tabacum*)	gi|8347420	=	–1.5	–4.6	–1.6	V	2	104	39.7/6.9	26.0/5.0
23	Glycyl tRNA synthetase, putative[a] (*N. benthamiana*)	gi|39863148	–1.7	=	=	=	M	3	105	81.9/6.6	80.0/6.9
24	Glycyl-tRNA synthetase (*A. thaliana*)	gi|110740563	<0.01	=	=	=	C	5	216	58/7.8	75.0/6.9
25	MPP β I subunit[a] (*N. tabacum*)	gi|92037471	=	=	=	1.5	M	9	482	60.0/6.2	60.0/6.3
26	MPP α II subunit[a] (*N. tabacum*)	gi|190874528	=	=	2	1.5	M	4	229	59.9/6.2	60.0/6.2
27	MPP α II subunit[a] (*N. tabacum*)	gi|76869884	–1.5	=	1.6	1.8	M	4	219	64.3/6.5	45.0/5.9

Table 1. *Continued*

Spot	Protein name	NCBI accession number	35 °C 3 h	35 °C 6 h	55 °C 3 h	55 °C 6 h	Loc.	MS/MS (Mascot) Pept./score	MW (Da)/pI Theor.	MW (Da)/pI Exp.
			Fold-of variation versus control							
28	P0 ribosomal protein-like[a] (*N. tabacum*)	gi|76866665	=	=	=	–2.6	Ch	2 116	33.9/5.1	35.0/5.2
29	Proteasome subunit β type-2-A[a] (*N. benthamiana*)	gi|47512323	=	=	=	2	C/N	9 493	28.0/9.3	23.0/6.8
30	20S proteasome α6 subunit (*N. benthamiana*)	gi|22947842	=	=	–1.8	–1.6	C/N	4 153	29.8/5.0	31.0/5.2
31	26S proteasome ATPase subunit RPT1 (*P. persica*)	gi|3914449	=	=	=	–2.1	C/N	3 183	48.0/6.4	48.0/6.2
32	Ubiquitin activating enzyme E1 (*N. tabacum*)	gi|1808656	=	=	–2	–2.7	C/N	2 114	121.3/5.3	120/5.3
33	Ubiquitin activating enzyme E2 (*N. tabacum*)	gi|38142361	=	=	–1.6	–3.2	C/N	3 121	121.2/5.0	120/5.3
34	SUMO1 (*A. thaliana*)	gi|15236885	=	=	=	–2.7	C	2 100	11.0/4.9	13.8/4.9
35	α7 proteasome subunit, putative (*N. tabacum*)	gi|14594925	=	=	2	=	C/N	8 321	27.2/6.1	18.0/5.9
Signal transduction/regulation										
36	65 kDa regulatory subunit of protein phosphatase 2A (*A. thaliana*)	gi|683506	1.6	=	=	=	C/M	3 120	65.6/5.0	64.0/5.0
37	14-3-3-like protein B (*N. tabacum*)	gi|3912948	=	=	–2.4	=	C	9 452	28.8/4.7	28.0/4.7
38	Arginine/serine-rich splicing factor binding protein[a] (*N. tabacum*)	gi|76869709	=	=	–2	<0.01	N	2 117	31.2/9.9	30.0/6.0
39	Novel calmodulin-like protein[c] (*O. sativa*)	gi|1235664	=	=	>100	=	N		21.0/4.75	22.0/4.7
40	Calmodulin[c] (*C. reinhardtii*)	gi|225024	=	=	>100	=	C	8 430	19.0/4.7	18.0/4.6
41	DEAD/DEAH box helicase, putative[b] (*V. vinifera*)	gi|225430261	1.6	=	=	=	C	5 190	48.9/5.4	48.5/5.7
42	Eukaryotic initiation factor 4–9 (*O. sativa*)	gi|303844	=	=	=	–2	C	5 211	47.0/5.3	48.0/5.5
43	Eukaryotic initiation factor 4A-11 (*N. tabacum*)	gi|2500518	=	=	–3.5	=	C	15 752	46.8/5.4	48.0/5.6
44	GTP binding protein RAN1 (*N. sylvestris*)	gi|48249480	=	=	=	–1.5	N	5 168	25.5/6.3	26.0/6.8
45	RAN GTPase-activating protein 2 (RanGAP2) (*N. benthamiana*)	gi|147882993	1.5	=	=	=	C	2 69	59.2/4.5	67.0/4.9
46	RNA Binding Protein 45 (*N. plumbaginifolia*)	gi|9663767	=	=	=	<0.01	N	3 80	45.2/5.9	49.8/6.4
47	SGT1 (*N. tabacum*)	gi|29468339	=	=	–3.2	=	C	4 142	41.4/5.2	33.0/5.4
48	Vernalization ind. 3-like protein[a] (*N. tabacum*)	gi|92020249	=	=	–2.1	=	C	3 220	35.0/5.8	35.0/5.7
Metabolism										
49	Betaine-aldehyde dehydrogenase[d] (*N. tabacum*)	gi|92037527	=	=	=	–2.2	M/Ch	3 187	59.7/5.4	57.3/5.6
50	Carboxylesterase[a] (*N. tabacum*)	gi|32871667	=	–1.5	=	–2.5	M/C/N	4 208	27.0/4.8	27.0/5.0
51	Enolase (*S. lycopersicum*)	gi|119354	–1.7	=	2	2.7	C	4 223	48.0/5.6	50.0/5.9
52	Enolase[c] (*L. luteus*)	gI|6996529	=	=	>100	=	C	9 316	47.0/6.0	48.0/6.4
53	Enolase[c] (*L. luteus*)	gI|6996529	=	=	>100	=	C	7 222	47.0/6.0	48.0/6.2

Table 1. *Continued*

Spot	Protein name	NCBI accession number	35 °C 3 h	35 °C 6 h	55 °C 3 h	55 °C 6 h	Loc.	MS/MS (Mascot) Pept.	MS/MS (Mascot) score	MW (Da)/pI Theor.	MW (Da)/pI Exp.
			Fold-of variation versus control								
54	GAPDH (*N. tabacum*)	gi|120676	=	=	–1.5	=	C	4	135	35.5/6.14	36.0/6.8
55	GRP-like protein 2[a] (*N. tabacum*)	gi|190730159	=	=	=	–1.7	C	3	122	40.1/6.0	40.5/6.7
56	Isovaleryl-CoA-dehydrogenase precursor (*A. thaliana*)	gi|5596622	=	=	1.5	1.8	M	3	144	44.7/7.5	43.4/6.2
57	Malate dehydrogenase[a] (*N. tabacum*)	gi|92028885	=	=	=	1.9	M	4	287	36.1/8.9	36.0/6.9
58	Methionine synthase (*S. tuberosum*)	gi|8439545	=	=	=	–1.5	C	7	276	84.7/6.0	95.0/6.4
59	Methionine synthase (*S. tuberosum*)	gi|8439545	–1.8	=	=	=	C	3	146	84.7/6.0	85.0/6.6
60	NADH-ubiquinone oxidoreductase 75 kDa sub. (*S. tuberosum*)	gi|3122572	=	=	=	1.6	M	11	574	80.8/5.9	85.0/6.1
61	NADH dehydrogenase, putative[a] (*N. benthamiana*)	gi|47232078	1.6	=	=	=	M	3	177	19.0/4.7	19.5/4.9
62	Nucleoside diphosphate kinase1 (*C. annuum*)	gi|12230332	2.3	=	=	=	C	2	110	16.3/6.3	16.3/6.3
63	Nucleoside diphosphate kinase 3[c] (*A. thaliana*)	gi|15237018	=	=	>100	=	M	5	215	17.0/6.8	16.9/6.9
64	Nucleoside diphosphate kinase 3[c] (*A. thaliana*)	gi|15237018	=	=	>100	=	M	5	210	17.0/6.8	17.0/6.5
65	Phosphoenolpyruvate carboxylase (*G. max*)	gi|399182	=	=	–1.7	=	C	2	74	110.6/5.7	110/5.8
66	Phosphoenolpyruvate carboxylase (*N. sylvestris*)	gi|20152209	=	=	=	2.1	C	2	116	86.3/6.3	100/6.3
67	Phosphoribosylaminoimidazolecarboxamide formyltransferase/IMP cyclohydrolase (*N. tabacum*)	gi|11878280	=	=	=	1.7	Ch	7	329	66.5/6.6	67.0/6.7
68	Putative beta-hydroxyacyl-ACP dehydratase[a] (*N. tabacum*)	gi|92011406	=	=	=	1.8	Ch	7	312	24.1/9.3	15.0/6.3
69	Pyridoxine biosynthesis protein isoform A, putative (*N. tabacum*)	gi|46399269	=	=	–2.7	–1.9	C	9	513	33.0/5.9	31.0/6.1
70	Pyruvate kinase, putative[a] (*N. tabacum*)	gi|83419369	=	=	–2.1	–3.7	Ch	3	137	64.0/6.9	66.0/6.2
71	Pyridoxine biosynthesis protein isoform A[a] (*N. tabacum*)	gi|46399269	=	=	–2.5	–1.8	Ch	3	146	33.4/5.9	31.0/5.9
72	Pyruvate decarboxylase isozyme 1 (*N. tabacum*)	gi|1706327	–1.5	=	=	–2	Ch	3	131	45.7/6.6	70/5.8
73	S-adenosylmethionine synthetase 2[a] (*N. tabacum*)	gi|76871648	=	=	–1.6	=	C	8	445	43.0/5.4	45.0/5.7
74	Spermidine synthase 1[a] (*N. tabacum*)	gi|92015347	=	=	–1.6	–2	C	6	335	34.6/5.5	34.0/5.2
75	Spermidine synthase 2[a] (*N. tabacum*)	gi|52837366	=	=	–1.8	=	C	2	85	34.4/5.2	33.0/5.5
76	UDP-glucose pyrophosphorylase[a] (*N. tabacum*)	gi|123209459	=	=	–2.6	=	C	7	458	51.8/5.4	50.0/6.7
77	Vacuolar H^+-ATPase β subunit (*N. tabacum*)	gi|6715512	=	=	=	1.9	V	8	351	53.8/5.1	55.0/5.1
78	α-1,4 glucan phosphorylase L-1 isozyme (*S. tuberosum*)	gi|21579	=	=	=	–2.5	Ch	3	135	110.0/5.4	110/5.4
79	α-1,4-glucan-protein synthase[a] (*N. tabacum*)	gi|123218663	=	=	2	1.5	C	7	337	42.5/6.2	39.0/5.9

Table 1. *Continued*

Spot	Protein name	NCBI accession number	35 °C 3 h	35 °C 6 h	55 °C 3 h	55 °C 6 h	Loc.	MS/MS (Mascot) Pept./score	MW (Da)/pI Theor.	MW (Da)/pI Exp.
			Fold-of variation versus control							
Secondary metabolism										
80	3-Hydroxy-3-methylglutaryl CoA synthase (*N. langsdorffii x N. sanderae*)	gi|157042747	=	=	–1.7	=	C	6 266	51.6/6.0	47.0/6.3
81	Chorismate synthase 1[a] (*N. tabacum*)	gi|123220736	=	=	–1.8	=	Ch	3 130	47.7/6.7	45.0/6.7
82	Sinapyl alcohol dehydrogenase (*N. tabacum*)	gi|89475491	=	=	–1.8	=	C	11 493	39.0/6.2	40.0/6.5
83	Tropinone reductase[a] (*N. tabacum*)	gi|92039116	1.5	=	–1.5	=	C	7 456	28.5/8.0	28.0/6.5
Cell structure										
84	Actin[a] (*S. tuberosum*)	gi|39805809	2	=	3	<0.01	Cs	8 310	41.8/5.3	43.0/5.4
85	Actin[a] (*S. tuberosum*)	gi|39805809	3.6	=	2.1	=	Cs	5 147	41.8/5.3	43.0/5.3
86	Actin[a] (*S. tuberosum*)	gi|39805809	=	=	2	=	Cs	3 142	41.8/5.3	43.0/5.2
87	Actin isoform B[a] (*N. benthamiana*)	gi|39877476	=	=	–2	–2.4	Cs	4 153	41.7/5.3	36.0/5.7
88	Actin (*N. tabacum*)	gi|197322805	=	=	–2.8	–3.2	Cs	2 71	41.7/5.3	35.0/5.7
89	Actin depolimerization factor 6[a] (*N. tabacum*)	gi|48757789	=	–1.5	=	–1.8	Cs	2 94	16.0/6.7	16.0/6.8
90	α-tubulin[a] (*N. tabacum*)	gi|17402467	=	=	<0.01	=	Cs	8 357	49.7/4.9	49.0/6.8
91	α-tubulin (*N. tabacum*)	gi|17402467	=	=	<0.01	=	Cs	8 307	49.7/4.9	49.0/6.9
92	α-tubulin (*N. tabacum*)	gi|11967906	=	=	–2.6	=	Cs	4 204	50.4/4.9	49.0/6.5
93	α-tubulin (*N. tabacum*)	gi|11967906	=	=	=	<0.01	Cs	2 124	50.4/4.9	49.0/5.2
94	α-tubulin (*N. tabacum*)	gi|11967906	=	=	–2.2	=	Cs	4 158	50.4/4.9	49.0/6.4

[a]Protein founded in the EST DataBase. The name, the molecular weight and the isoelectric point of the protein were annotated by BLAST search.
[b]Protein unknown annotated by BLAST search.
[c]Protein identified only in NCBI DataBase 'All' annotated by BLAST search against viridiplantae.
[d]Protein confirmed by *de novo* analysis.
Significant matches had a Molecular Weight Search (Mowse) score greater than 49 or 69 for EST ($P < 0.05$).
The value '>100' ('<0.01') means that the protein spot is detected (is not present) exclusively under the condition reporting this value.
C, cytoplasm; N, nucleus; V, vacuole; Ch, chloroplast; M, mitochondrion; Cs, cytoskeleton.

the 55 °C treatment, we observed a drop in the level of free SUMO and a concomitant strong increase in SUMO-conjugated proteins.

Effects of the recovery of spermidine biosynthesis on ascorbate peroxidase suppression and PCD occurrence

As the proteomic studies showed a down-accumulation of spermidine biosynthesis-related proteins, the effects of exogenous addition of spermidine on PCD were also analysed. Our results show that spermidine protected the HS-exposed cells from PCD in a dose-dependent manner (Fig. 5a). As a remarkable suppression of APX has been reported to occur as an early event in PCD (Vacca *et al.* 2004; Locato *et al.* 2008), the activity of this enzyme was also tested after PCD induction in the spermidine-enriched cells. Pre-treatment with spermidine also significantly rebounded APX suppression in a dose-dependent manner (Fig. 5b).

DISCUSSION

The present study investigated the changes of proteome patterns in TBY-2 cells under two different heat stresses,

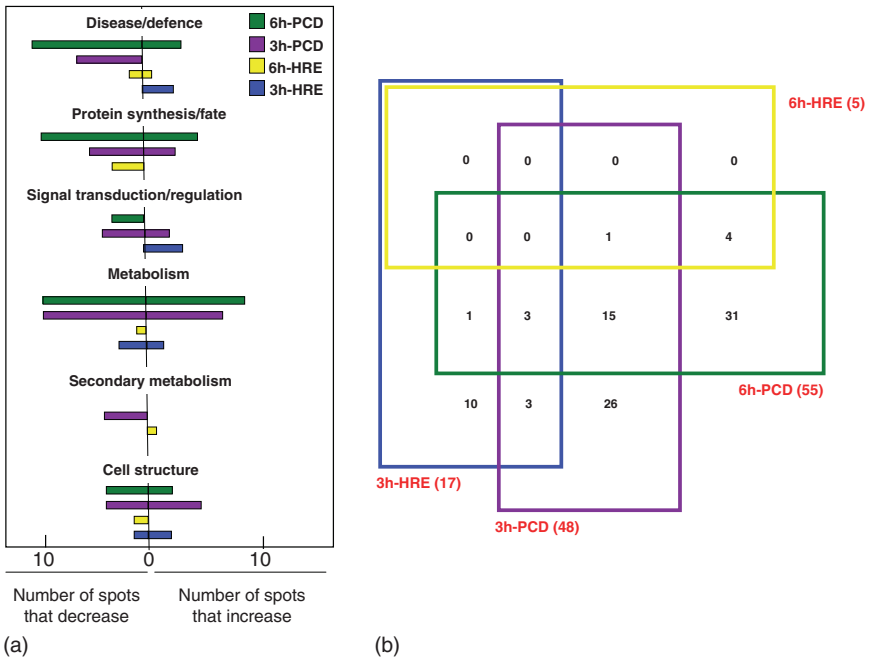

Figure 2. (a) Functional classification of proteins that change significantly (*t*-test; $P < 0.05$) in relative abundance of at least 1.5-fold between control and heat treated cells. (b) Venn diagram showing the degree of overlap between significantly regulated proteins from 3 h-homeostatic response (HRE; blue), 6 h-HRE (yellow), 3 h-PCD (purple) and 6 h-PCD cells (green). In parentheses is indicated the sum of all up- and down-accumulated proteins for each condition.

namely 10 min exposure at 35 and 55 °C; these treatments were able to induce HRE and PCD, respectively. A large number of proteins differentially-accumulated under the two stress conditions were identified, with the most relevant changes concerning 3 to 6 h-PCD cells. Changes associated with heat- and senescence-induced PCD have also been identified by proteomic studies in Arabidopsis cell suspension cultures (Swidzinski *et al*. 2004). This previous study reported results different to ours, probably because the experimental systems analysed were different in term of plant species, time of analysis after PCD induction (immediate analysis versus 3 or 6 h after HS treatment) and 2-DE set-up.

Quantitative data revealed that only a minor overlap of differentially-accumulated proteins was evident between HRE and PCD. This indicates that the different severity of heat treatment induced the modulation of specific proteins belonging to different categories, some of which are responsible for the different cell fates (Fig. 6).

Detoxifying and antioxidant enzymes

In 3 h HRE cells, two proteins involved in oxidative stress were accumulated: a NADPH-dependent thioredoxin reductase (spot 18); and a cytosolic APX (spot 2). Both these enzymes are involved in redox homeostasis, thus underlining the importance of redox balance for cellular survival. The accumulation of APX strongly supports previous results indicating that the oxidative stress triggered by 35 °C HS induces a rise in the cytosolic APX expression and activity, aimed at restoring the ROS impairment caused by heat stress (Dat *et al*. 2003; Suzuki & Mittler 2006; Locato *et al*. 2009). On the other hand, when the stress level was higher (at 55 °C HS), a decrease in cytosolic APX occurred, as the two spots corresponding to this isoenzyme (spots 2 and 3) were both found to be decreased. It is interesting to observe that spot 2 appears to recover in 6 h-PCD cells. The decrease in APX was inhibited by pre-treatment with spermidine, a treatment that also reduces the occurrence of PCD (see further discussion). Consistently, a decrease in the activity of cytosolic APX has been suggested to contribute to the oxidative burst characterizing PCD, even acting as a very early event in the signalling pathway leading to PCD (Panavas & Rubinstein 1998; Mittler *et al*. 1999; Fath *et al*. 2001, de Pinto *et al*. 2002, 2006; Vacca *et al*. 2006). Therefore, the proteomic data confirm the pivotal role of cytosolic APX in heat-stress responses.

In 6 h-PCD cells, a decrease in ferritin-1 protein (spot 8) was also observed. Recent data suggest that control of ferritin synthesis is required for proper maintenance of the cellular redox status (Ravet *et al*. 2009).

Among the proteins involved in ROS detoxification and redox balance, the strongest decrease was for a thioredoxin peroxidase (spot 19). Two spots (69 and 70) with high homology to pyridoxine biosynthesis protein isoform A also exhibited significantly-decreased expression. Vitamin B6 is a potent antioxidant with a particular ability to quench superoxide and singlet oxygen. The *Arabidopsis* pyridoxine biosynthesis genes (*PDX1* and *PDX2*) are up-regulated by abiotic stressors suggesting that vitamin B6 plays an important role in oxidative stress responses (Denslow *et al*. 2007). Moreover, pyridoxal treatment has been shown to suppress apoptosis in mammalian cells through its antioxidant effects (Endo *et al*. 2007). Two enzymes involved in spermidine biosynthesis (spots 74 and 75) and an enzyme that catalyses glycine betaine synthesis (spot 49) were significantly decreased in 55 °C-treated cells. Results from previous investigations suggest that exogenous application of spermidine and glycine betaine is able to alter the expression or activity of some scavenging enzymes as well as the cellular

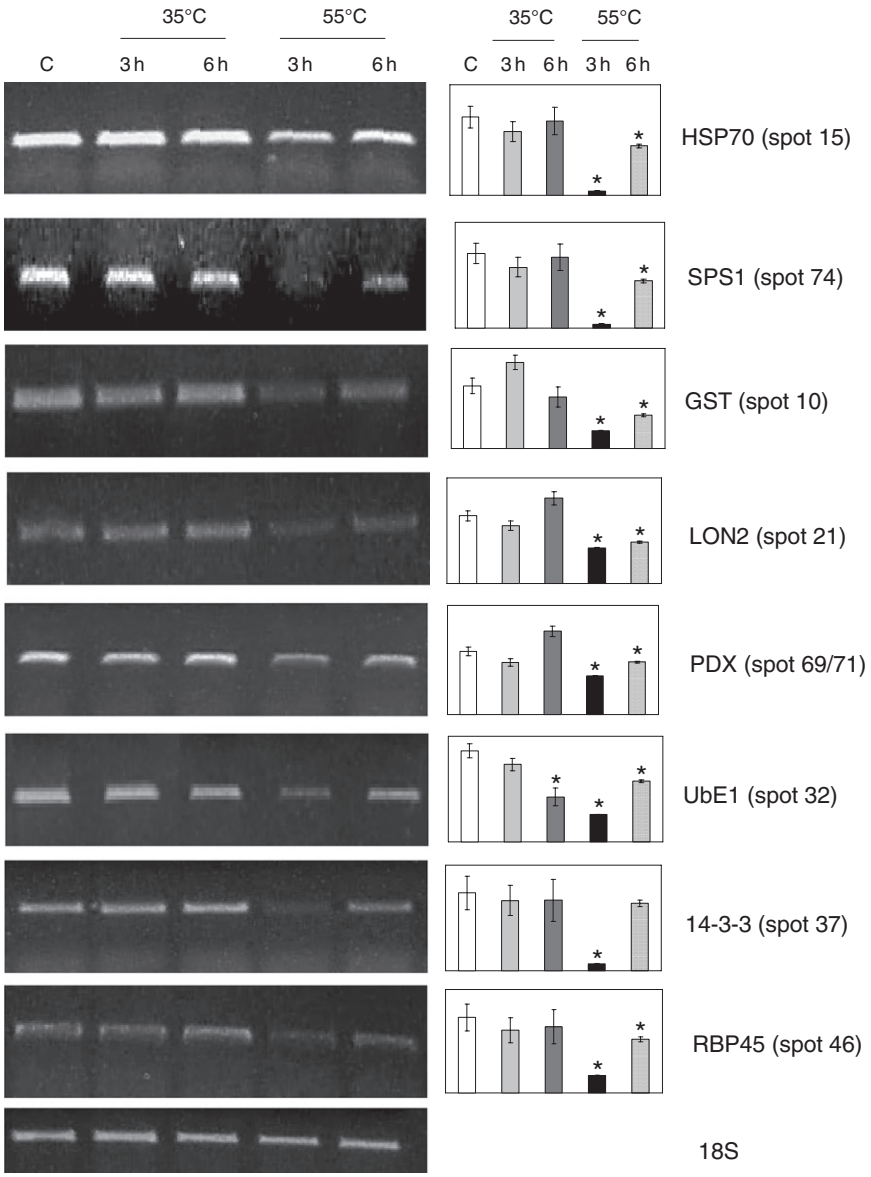

Figure 3. RT-PCR expression analysis of selected genes that displayed differential accumulation on 2D protein maps (Fig. 1). Total RNA was extracted from non-treated cells (C) and samples collected 3 and 6 h after 35 and 55 °C heat treatments. The housekeeping gene 18S rRNA, which displays constitutive expression in all samples, was used as internal control. * indicates values that are significantly different from control cells with $P < 0.05$ (Student's *t*-test).

levels of ROS, thus modifying the oxidative stress intensity (Park *et al*. 2004; He *et al*. 2008). As already mentioned, a similar effect of spermidine was also evident on APX in our experimental system.

In the 55 °C-treated cells, the two glutathione S-transferases (spots 10 and 11) were down-accumulated. This might be correlated with the strong decrease in glutathione availability occurring during HS-dependent PCD, as the glutathione content of 3 h-PCD and 6 h-PCD cells is about 30 and 50% lower, respectively, than of control cells (Locato *et al*. 2008).

The proteomic picture showing the down-accumulation of different proteins involved in cellular redox homeostasis could provide an important, and until now unappreciated, contribution to understanding how many partners are involved in promoting the redox impairment leading to PCD.

Different mechanisms are involved in controlling the protein fate in cells undergoing PCD. In PCD cells, significant changes in the accumulation of some subunits of the proteasome system were found, namely the increase of β2 (spot 29), and a fragment of α7 (spot 35) and the decrease of RPT1 (spot 31) and α6 (spot 30). The reduced expression of α6 has been shown to be essential for activating the PCD pathway in *Nicotiana benthamiana* (Kim *et al*. 2003). The latter two subunits (RTP1 and α6) have been recently found to be degraded by caspase-7 during apoptosis in the MCF-7 human cell line (Jang *et al*. 2007). The results reported here suggest that these two subunits could also be substrates for caspase-like activities in plants. The different behaviour of the proteins involved in proteasome structure and activity during PCD suggests that the cleavage of specific subunits could be relevant in controlling proteasome activity and driving cells

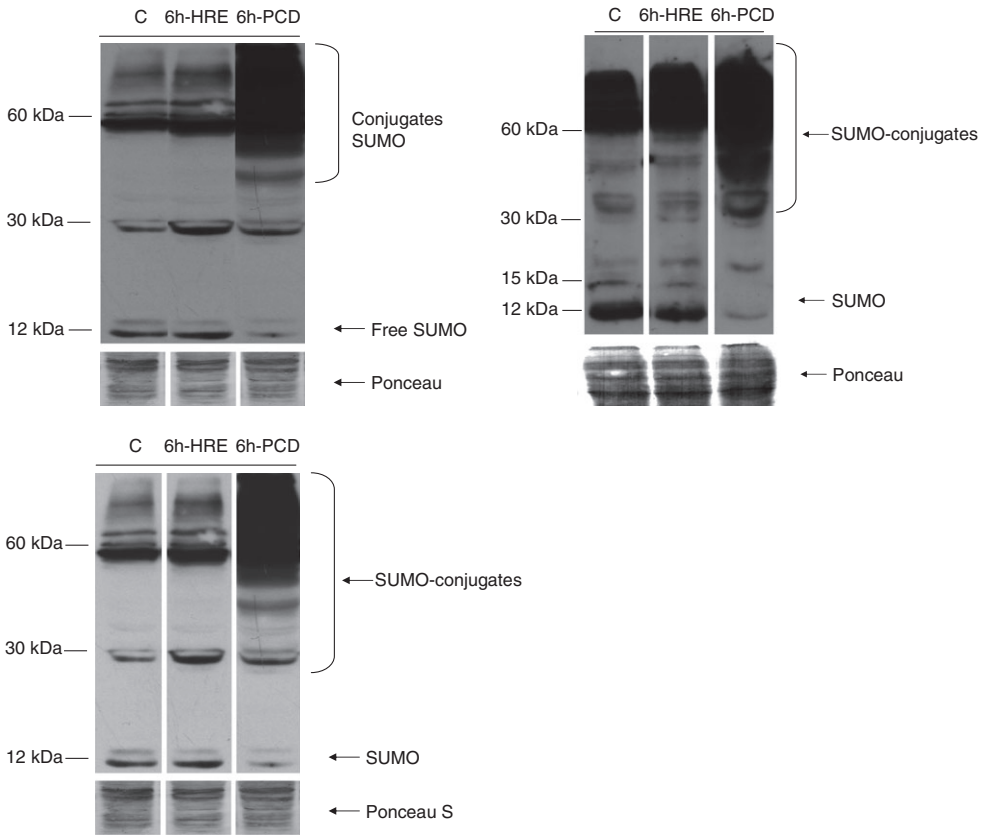

Figure 4. Western blot analysis with small ubiquitin-like modifier-1 (SUMO-1) antibody detecting Sumo protein and Sumoylated conjugates in control sample (C); in cells exposed to 35 °C for 10 min and then recovered for 6 h at 27 °C (6 h-HRE); in cells exposed to 55 °C for 10 min and then recovered for 6 h at 27 °C (6 h-PCD). Arrowhead indicates free SUMO-1. Membrane Ponceau staining was used for loading control. HRE, homeostatic response; PCD, programmed cell death.

toward irreversible PCD. This point requires further investigation.

Protein degradation is also controlled by the ubiquitination-related enzymes E1, E2 and E3. The down-accumulation of the enzymes E1 and E2 found in PCD-induced cells (spots 32 and 33) can lead to incorrect tagging of the proteins to be degraded by ubiquitin. In animal cells, a temperature-sensitive defect in the ubiquitin-activating E1 enzyme induces apoptosis (Monney *et al*. 1998). Our data revealed changes in the level of Lon2 protease (spot 21). This enzyme degrades oxidatively-modified proteins in the mitochondrial matrix (a function similar to that of the 20S proteasome in the cytoplasm) and plays a key role in the maintenance of mitochondrial homeostasis under stress conditions (Ngo & Davies 2007). In animal cells, Lon protease expression and activity decline with age and this may contribute to the accumulation of the oxidatively modified protein aggregates typically observed in aging and diseased cells. Complete loss of Lon activity leads to apoptosis (Bota *et al*. 2005).

Proteomic analysis revealed the down-accumulation in 6 h-PCD of SUMO1. Western blot analysis indicates a differential involvement of the sumoylation process in the cell response to the different heat intensities. In cells collected 6 h after being exposed to 35 °C for 10 min, the levels of SUMO protein and SUMO conjugates are similar to control cells. This result is consistent with data obtained by Kurepa *et al*. (2003) in Arabidopsis plants treated at 37 °C. In cells collected 6 h after being exposed to 55 °C for 10 min, a marked accumulation of SUMO conjugates is observed, with a concomitant drop in the levels of free SUMO.

Differential modulation of the subunits of mitochondrial processing peptidase (MPP, spots 25, 26 and 27) was also found, with down-accumulation in HRE-cells and up-accumulation in PCD-cells. Most mitochondrial proteins are synthesized as precursor proteins with extension peptides. After their import into mitochondria, the extension peptides are cleaved off by MPP, allowing the targeted proteins to acquire their final conformation and functionality. The observed changes in MPP could occur as a downstream consequence of variations in the amount of protein imported into mitochondria, or may be a mechanism that contributes to regulation of the metabolism of this organelle that plays a pivotal role in PCD signalling. To our knowledge, the involvement of MPP in the transduction pathways leading to PCD has never been taken into account.

Collectively, our data suggest that post-translational modifications (such as sumoylation or MPPase) and protein degradation (e.g. through the ubiquitin-proteasome pathway) are part of a coordinated network of events

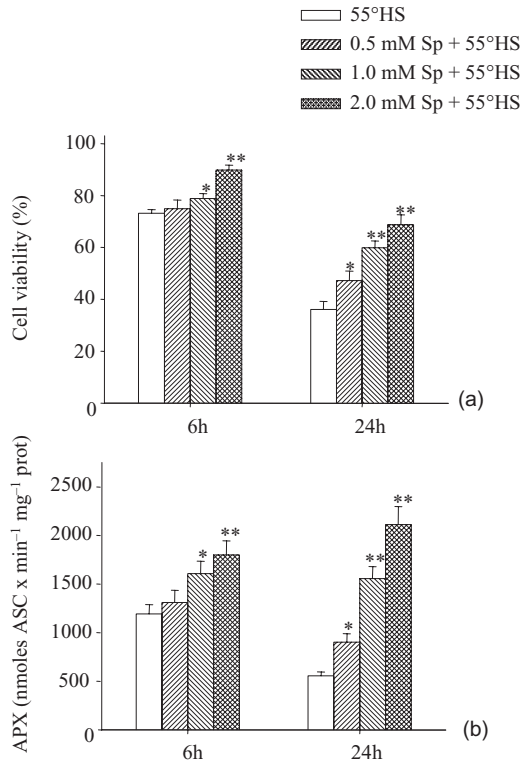

Figure 5. Effect of spermidine pre-treatment on (a) cell viability and (b) ascorbate peroxidase (APX) activity in programmed cell death (PCD)-induced by 55 °C heat shock (HS). Different concentrations of spermidine were added to the culture medium 15 min before the HS exposition. The values are the means of three different experiments ± standard deviation. * and ** indicates values that are significantly different from control cells with $P < 0.05$ and $P < 0.01$, respectively (Student's *t*-test).

affecting the turnover of specific proteins and playing important roles in the adaptation of TBY-2 cells to different heat stresses. Determining how the two different HSs activate these events, and identifying the various targets, will be important to determine their relevance in controlling the cell fate under heat stress.

Differential accumulation of proteins related to regulation

The levels of most proteins in this category were modified 3 h after heat treatment, which supports their function in cell signalling. In 3 h-HRE cells, a putative DEAD/DEAH box helicase (spot 41) was increased. The role of these helicases in stress responses of plants has only just begun to be understood: a DEAD-box RNA helicase with functions in modulating oxidative stress has been recently reported (Li *et al*. 2008). We found two proteins related to Ran's GTPase activity (spots 44 and 45) that have opposite behavior depending on the severity of the heat stress. The small GTPase Ran proteins are the central element of a conserved signalling network that has a prominent role in mitotic regulation. Acute silencing of Ran in various types of tumor cells causes aberrant mitotic spindle formation, mitochondrial dysfunction and apoptosis (Xia *et al*. 2008). The over-expression of Ran1 of wheat increases the proportion of cells in G2 phase and causes an elevated mitotic index and prolonged life cycle (Wang *et al*. 2006).

Differential accumulation of proteins related to metabolism

Numerous studies have demonstrated that cell survival and death are related to glucose metabolism and that apoptosis is partially dependent on energy status (Azad *et al*. 2008). In the present study, expression levels of several enzymes of carbohydrate metabolism (GAPDH, spot 54, PK, spot 71, malate dehydrogenase, spot 57 and phosphoenolpyruvate carboxylase, spots 65 and 66) were found to be altered in PCD cells. The decrease in pyruvate kinase and the increase in enolase, PEPase and malate dehydrogenase seem to suggest stimulation of the tricarboxylic acid (TCA) cycle in HS-PCD cells; this could represent a sort of compensation for the decrease in mitochondrial respiration efficiency that occurs in TBY-2 cells undergoing HS-PCD (Vacca *et al*. 2004; Valenti *et al* 2007).

Interestingly, in 6 h-PCD cells we found an increase in IMP cyclohydrolase (spot 67), an enzyme involved in *de novo* purine biosynthesis. It was shown previously that changes in purine and pyrimidine content are early metabolic events of the cell death programme in TBY-2 (Stasolla *et al*. 2005).

Several proteins involved in nucleotide-sugar metabolism and the cell wall are modified by the two heat treatments. In 3 h-PCD we found a decrease in the level of UDP-glucose phosphorylase (UGPase, spot 76), an enzyme that catalyses the reversible production of UDP-glucose and pyrophosphate from Glc-1-P and UTP. UGPase occupies a critical position at the crossroad of Suc synthesis/breakdown. The down-accumulation of this enzyme may result in a greater availability of glucose for glycolysis and UTP for the synthesis of ATP. Our proteomic data indicated that two nucleoside diphosphate kinases (NDPK) were subjected to differential modulation, according with the different fate that the cells must follow. In 3 h HRE cells we observed accumulation of the cytoplasmic NDPK1 isoform (spot 62). In *Arabidopsis*, NDPK1 is a component of ROS signaling through its interaction with three catalases (Fukamatsu *et al*. 2003). On the other hand, the mitochondrial NDPK3 isoform (spot 63 and 64) was up-regulated in 3 h-PCD cells. It has been suggested that during the process of PCD, this protein migrates to the nucleus where it executes a DNAse function (Hammergren *et al*. 2007). This situation may be similar to that in animals, but further investigation is needed to elucidate the possible involvement of the different isoforms of NDPKs in plant PCD.

CONCLUSION

The overall picture that emerges from this study is that two markedly different types of metabolic change are involved

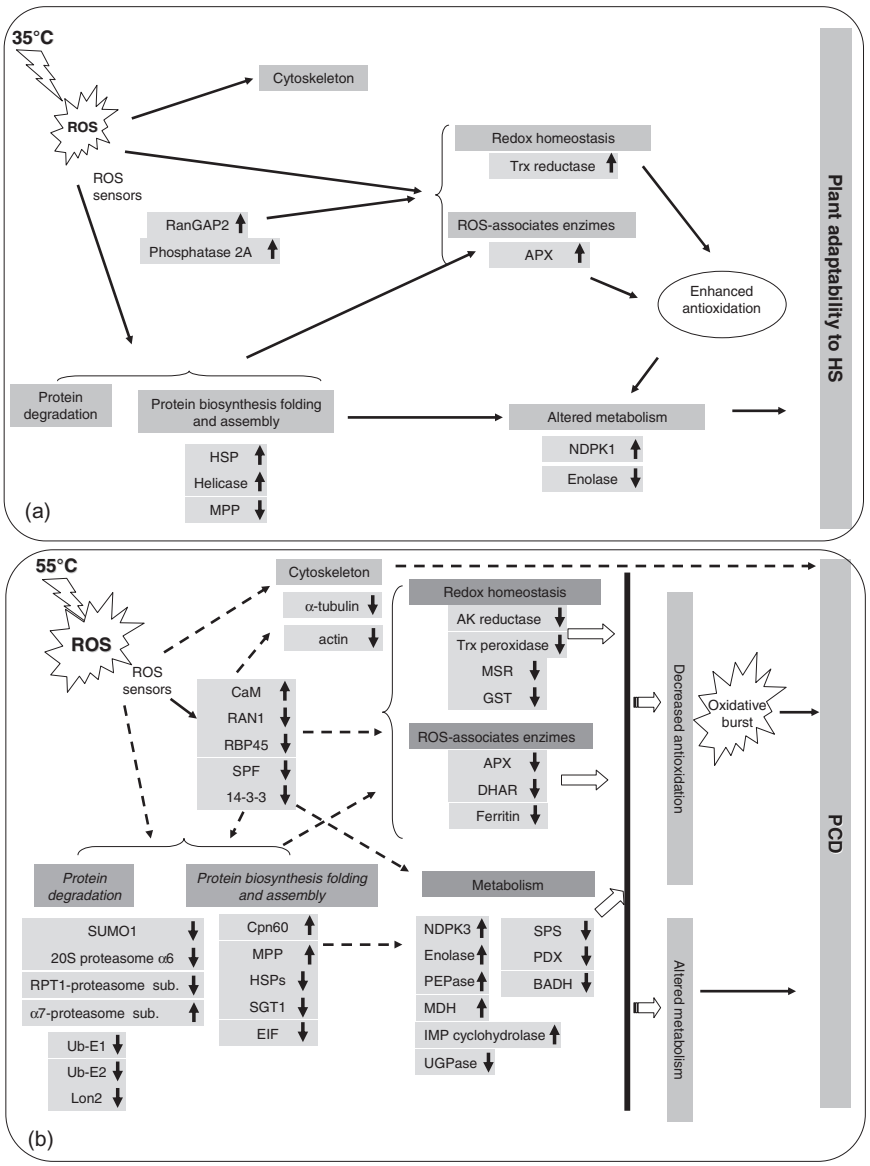

Figure 6. A putative model of the response of tobacco Bright Yellow-2 (TBY-2) cells 6 h after the 35 °C (a) and 55 °C (b) heat stress. Only some of the heat shock (HS) responsive proteins are indicated with those up-accumulate marked by ↑ and those down-accumulate marked by ↓. *MDH*, malate dehydrogenase; *NDPK*, nucleoside diphosphate kinase; *MPP*, mitochondrial processing peptidase; *PEPase* phosphoenolpyruvate carboxylase; *UGP-ase*, UDP-glucose pyrophosphorylase; *PDX*, pyridoxine biosynthesis protein isoform A, putative; *RanGAP2*, RAN GTPase-activating protein 2; *RBP45*, RNA Binding Protein 45; *SPS*, spermidine synthase; *BADH*, betaine-aldehyde dehydrogenase; *MSR*, methionine sulfoxide reductase; DHAR, dehydroascorbate reductase; *EIF*, eukaryotic initiation factor; *SPF*, arginine/serine-rich splicing factor binding protein; *Trx*, thioredoxin.

in the adaptation of TBY-2 cells to different intensities of heat stress (Fig. 6). When the imposed heat shock is beyond a certain threshold, the overall reduced metabolism may be the result of a series of events in gene expression and oxidative damage that would lead to PCD. Based on their putative functions and on previously published results, we suggest that some of the 55 °C-responsive proteins play a pivotal role in inducing cells to 'commit suicide'. In particular, our data seem to suggest that the down-accumulation of several proteins involved in antioxidant activity contributes to the oxidative burst characterizing HS-PCD. These results may deepen our understanding of the sophisticated functional network for regulation of the oxidative stress in HS-induced PCD. To elucidate the role in HS-PCD of the other differentially-accumulated proteins, further functional research is necessary. However, our findings underline the potential of the proteomic approach for understanding the involvement of newly-identify pathways and their relationship to a particular process.

SUPPORTING INFORMATION AVAILABLE

Specific primers used for RT-PCR of genes encoding the changed proteins identified by 2-DE analysis, key for loci in the four-way Venn diagram.

ACKNOWLEDGMENTS

We would like to thank Dr. E. Mazzucotelli for her suggestions on Western analysis of SUMO proteins. This research was partially supported by the Italian Ministry of University and Research (PRIN n. 20084XTFBC).

REFERENCES

Aina R., Labra M., Vannini C., Marsoni M., Cucchi U., Bracale M., Sgorbati S., Fumagalli P. & Citterio S. (2007) Thiol peptide level and proteomic changes in response to cadmium toxicity in Oryza sativa L. root. *Environmental and Experimental Botany* **59,** 381–392.

Azad A., Ishikawa T., Ishikawa T., Sawa Y. & Shibata H. (2008) Intracellular energy depletion triggers programmed cell death during petal senescence in tulip. *Journal of Experimental Botany* **59,** 2085–2095.

Baena-González E. & Sheen J. (2008) Convergent energy and stress signaling. *Trends in Plant Science* **13,** 274–482.

Baniwal S., Bharti K., Chan K., *et al*. (2004) Heat stress response in plants: a complex game with chaperones and more than twenty heat stress transcription factors. *Journal of Biosciences* **29,** 471–487.

Bates B.C., Kundzewicz Z.W., Wu S. & Palutikof J.P. (eds) (2008) *Climate Change and Water*. Technical Paper of the Intergovernmental Panel of Climate Change. IPCC Secretariat, Geneva, Switzerland.

Bevan M., Bancroft I., Bent E., *et al*. (1998) Analysis of 1.9 Mb of contiguous sequence from chromosome 4 of *Arabidopsis thaliana*. *Nature* **391,** 485–488.

Bota D., Ngo J. & Davies K. (2005) Downregulation of the human Lon protease impairs mitochondrial structure and function and causes cell death. *Free Radical Biology & Medicine* **38,** 665–677.

Burbridge E., Diamond M., Dix P. & McCabe P. (2007) Use of cell morphology to evaluate the effect of a peroxidase gene on the cell death induction thresholds in tobacco. *Plant Science* **172,** 853–860.

Challinor A.J., Ewert F., Arnold S., Simelton E. & Fraser E. (2009) Crops and climate change: progress, trends and challenges in simulating impacts and informing adaptation. *Journal of Experimental Botany* **60,** 2775–2789.

Dat J.F., Pellinen R., Beeckman T., Van De Cotte B., Langebartels C., Kangasjarvi J., Inzé D. & Van Breusegem F. (2003) Changes in hydrogen peroxide homeostasis trigger an active cell death process in tobacco. *The Plant Journal* **33,** 621–632.

Delledonne M., Xia Y., Dixon R. & Lamb C. (1998) Nitric oxide functions as a signal in plant disease resistence. *Nature* **394,** 585–588.

Denslow S., Reuschhoff E. & Daub M. (2007) Regulation of the *Arabidopsis thaliana* vitamin B6 biosynthesis genes by abiotic stress. *Plant Physiology and Biochemistry* **45,** 152–161.

Desikan R., Mackerness S., Hancock J. & Neill S. (2001) Regulation of the *Arabidopsis* trascriptome by oxidative stress. *Plant Physiology* **127,** 159–172.

Endo N., Nishiyama K., Okabe M., Matsumoto M., Kanouchi H. & Oka T. (2007) Vitamin B_6 suppresses apoptosis of NM-1 bovine endothelial cells induced by homocysteine and copper. *Biochimica et Biophysica Acta* **1770,** 4571–4577.

Fath A., Bethke P. & Russell L. (2001) Enzymes that scavenge reactive oxygen species are down-regulated prior to gibberellic acid-induced programmed cell death in barley aleurone. *Plant Physiology* **126,** 156–166.

Fukamatsu Y., Yabe N. & Hasunuma K. (2003) *Arabidopsis* NDK1 is a component of ROS signaling by interacting with three catalases. *Plant & Cell Physiology* **44,** 982–989.

Gadjev I., Stone J. & Gechev T. (2008) Programmed cell death in plants: new insights into redox regulation and the role of hydrogen peroxide. *International Review of Cell & Molecular Biology* **270,** 88–144.

Hammergren J., Sundstrom J., Johansson M., Bergman P. & Knorpp C. (2007) On the phylogeny, expression and targeting of plant nucleoside diphosphate kinase. *Physiologia Plantarum* **129,** 79–89.

He L., Ban Y., Inoue H., Matsuda N., Liu J. & Moriguki T. (2008) Enhancement of spermidine content and antioxidant capacity in transgenic pear shoots overexpressing apple spermidine synthase in response to salinity and hyperosmosis. *Phytochemistry* **69,** 2133–2141.

Jang M., Park B., Lee A., *et al*. (2007) Caspase-7 mediated cleavage of proteasome subunits during apoptosis. *Biochemical and Biophysical Research Communications* **363,** 388–394.

Kim M., Ahn J., Jin U.-H., Paek K.-H. & Pai H.-S. (2003) Activation of the programmed cell death pathway by inhibition of proteasome function in plants. *The Journal of Biological Chemistry* **278,** 19406–19415.

Kurepa J., Wolker J.M., Smalle J., Gosink M.M., Davis S.J., Durham T.L., Sung D.J. & Viestra R.D. (2003) The small ubiquitin –like modifier (SUMO) protein modification system in *Arabidopsis*. *The Journal of Biological Chemistry* **278,** 6862–6872.

Li D., Liu H., Zhang H., Wang X. & Song F. (2008) OsBIRH1, a DEAD-box RNA helicase with functions in modulating defense responses against pathogen infection and oxidative stress. *Journal of Experimental Botany* **59,** 2133–2146.

Locato V., Gadaleta C., De Gara L. & de Pinto M. (2008) Production of reactive species and modulation of antioxidant network in response to heat shock: a critical balance for cell fate. *Plant, Cell & Environment* **31,** 1608–1619.

Locato V., de Pinto M. & De Gara L. (2009) Different involvement of the mitochondrial, plastidial and cytosolic ascorbate-glutathione redox enzymes in heat shock responses. *Physiologia Plantarum* **135,** 296–306.

Marsoni M., Bracale M., Espen L., Prinsi B., Negri A.S. & Vannini C. (2008) Proteomic analysis of somatic embryogenesis in *Vitis vinifera*. *Plant Cell Reports* **27,** 347–356.

Mittler R. & Lam E. (1995) In situ detection of nDNA fragmentation during the differentiation of tracheary elements in higher plants. *Plant Physiology* **108,** 489–493.

Mittler R., Herr E., Orvar B.L., van Camp W., Willekens H., Inzé D. & Ellis B. (1999) Transgenic tobacco plants with reduced capability to detoxify reactive oxygen intermediates are hypersensitive to pathogen infection. *Proceedings of the National Academy of Sciences of the United States of America* **96,** 14165–14170.

Monney L., Otter I., Olivier R., Ozer H., Haas A., Satoshi Omura L. & Borner C. (1998) Defects in the ubiquitin pathway induce caspase-independent apoptosis blocked by Bcl-2. *Biological Chemistry* **273,** 6121–6131.

Ngo J. & Davies K. (2007) Importance of the lon protease in mitochondrial maintenance and the significance of declining lon in aging. *Annals of the New York Academy of Sciences* **1119,** 78–87.

Panavas T. & Rubinstein B. (1998) Oxidative events during programmed cell death of daylily (*Hemerocallis* hybrid) petals. *Plant Science* **133,** 125–138.

Park E.J., Jeknic Z., Sakamoto A., DeNoma J., Yuwansiri R., Murata N. & Chen T.H.H. (2004) Genetic engineering of glycinebetaine synthesis in tomato protects seeds, plants and flowers from chilling damage. *The Plant Journal* **40,** 474–487.

de Pinto M.C., Tommasi F. & De Gara L. (2002) Changes in the antioxidant systems as part of the signaling pathway responsible for the programmed cell death activated by nitric oxide and reactive oxygen species in tobacco BY-2 cells. *Plant Physiology* **130,** 698–708.

de Pinto M.C., Paradiso A., Leonetti P. & De Gara L. (2006) Hydrogen peroxide, nitric oxide and cytosolic ascorbate peroxidase at the crossroad between defence and cell death. *The Plant Journal* **48,** 784–795.

Porter J.R. & Semenov M.A. (2005) Crop response to climatic variation. *Philosophical Transactions of the Royal Society of London. Series B, Biological Sciences* **360,** 2021–2038.

Ravet K., Touraine B., Boucherez J., Briat J.F., Gaymard F. & Cellier F. (2009) Ferritins control interaction between iron homeostasis and oxidative stress in *Arabidopsis*. *The Plant Journal* **57,** 400–412.

Scott I. & Logan D. (2008) Mitochondrial morphology transition is an early indicator of subsequent cell death in *Arabidopsis*. *The New Phytologist* **17,** 90–101.

Stasolla C., Loukanina N., Yeung E. & Thorpe T. (2005) Progression of programmed cell death in tobacco BY-2 cells is delineated by specific changes in de novo and salvage synthesis of purine nucleotides. *Physiologia Plantarum* **123,** 254–261.

Suzuki N. & Mittler R. (2006) Reactive oxygen species and temperature stresses: a delicate balance between signaling and destruction. *Physiologia Plantarum* **126,** 45–51.

Swidzinski J.A., Leaver C.J. & Sweetlove L.J. (2004) A proteomic analysis of plant programmed cell death. *Phytochemistry* **65,** 1829–1838.

Vacca R.A., de Pinto M.C., Valenti D., Passerella S., Marra E. & De Gara L. (2004) Production of reactive oxygen species, alteration of cytoplasmic ascorbate peroxidase, and impairment of mitochondrial metabolism are early events in heat shock-induced programmed cell death in tobacco bright-yellow 2 cells. *Plant Physiology* **134,** 1100–1112.

Vacca R.A., Valenti D., Bobba A., Merafina R., Passarella S. & Marra E. (2006) Cytochrome c is released in a reactive oxygen species-dependent manner and is degraded via caspase-like proteases in tobacco Bright-Yellow 2 cells en route to heat shock-induced cell death. *Plant Physiology* **141,** 208–219.

Valenti D., Vacca R., de Pinto M.C., De Gara L., Marra E. & Passarella S. (2007) In the early phase of programmed cell death in Tobacco Bright Yellow 2 cells the mitochondrial adenine nucleotide translocator, adenylate kinase and nucleoside diphosphate kinase are impaired in a reactive oxygen species-dependent manner. *Biochim Biophys Acta* **1767,** 66–78.

Wang H., Li J., Bostock R. & Gilchrist D. (1996) Apoptosis: a functional paradigm for programmed plant cell death induced by a hostselective phytotoxin and invoked during development. *The Plant Cell* **8,** 375–391.

Wang X., Xu Y., Han Y., Bao S., Du J., Yuan M., Xu Z. & Chong K. (2006) Overexpression of RAN1 in rice and *Arabidopsis* alters primordial meristem, mitotic progress, and sensitivity to auxin. *Plant Physiology* **140,** 91–101.

Xia F., Lee C. & Altieri D. (2008) Tumor cell dependence on ran-GTP–directed mitosis. *Cancer Research* **68,** 1826–1833.

Yu C.S., Chen Y.C., Lu C.H. & Hwang J.K. (2006) Prediction of protein subcellular localization. *Proteins: Structure, Function and Bioinformatics* **64,** 643–651.

Received 30 November 2009; received in revised form 28 January 2010; accepted for publication 29 January 2010

SUPPORTING INFORMATION

Additional Supporting Information may be found in the online version of this article:

Figure S1. Four-way Venn diagram analysis for significantly regulated proteins from HRE and PCD cells compared with the control. (a) Key for loci in the four-way Venn diagram in Fig. 2, (b) numbers corresponding to the spot of the Table 1.

Table S1. Specific primers used for RT-PCR of genes encoding the changed proteins identified by 2-DE analysis.

Please note: Wiley-Blackwell are not responsible for the content or functionality of any supporting materials supplied by the authors. Any queries (other than missing material) should be directed to the corresponding author for the article.